nature structural & molecular biology

Structure of an RNA polymerase II–RNA inhibitor complex elucidates transcription regulation by noncoding RNAs

Hubert Kettenberger[1,3], Alexander Eisenführ[2], Florian Brueckner[1], Mirko Theis[2], Michael Famulok[2] & Patrick Cramer[1]

The noncoding RNA B2 and the RNA aptamer FC bind RNA polymerase (Pol) II and inhibit messenger RNA transcription initiation, but not elongation. We report the crystal structure of FC*, the central part of FC RNA, bound to Pol II. FC* RNA forms a double stem-loop structure in the Pol II active center cleft. B2 RNA may bind similarly, as it competes with FC* RNA for Pol II interaction. Both RNA inhibitors apparently prevent the downstream DNA duplex and the template single strand from entering the cleft after DNA melting and thus interfere with open-complex formation. Elongation is not inhibited, as nucleic acids prebound in the cleft would exclude the RNA inhibitors. The structure also indicates that A-form RNA could interact with Pol II similarly to a B-form DNA promoter, as suggested for the bacterial transcription inhibitor 6S RNA.

A recently discovered mechanism for gene regulation involves noncoding RNAs that bind and inhibit cellular RNA polymerases. Mouse B2 RNA, a 178-mer noncoding RNA transcribed by Pol III, binds Pol II and inhibits transcription of protein-coding genes during heat shock[1,2]. In *Escherichia coli* and apparently in many other bacteria, 6S RNA binds RNA polymerase and inhibits transcription of housekeeping genes upon entry into stationary cell growth[3–5]. Understanding how these RNAs inhibit transcription requires their three-dimensional structures in complex with the target polymerases, but neither mouse Pol II nor *E. coli* RNA polymerase is currently amenable to crystallographic analysis. To study inhibition of a cellular RNA polymerase by RNA, we used Pol II from the yeast *Saccharomyces cerevisiae*, which is well suited for structural studies, and a previously described 80-nucleotide RNA aptamer that binds and inhibits yeast Pol II, termed RNA FC[6]. Here we report the crystal structure of yeast Pol II in complex with the central region of FC RNA. Together with biochemical data and published results, the structure has implications for understanding the inhibitory mechanisms of polymerase-binding RNAs.

RESULTS

Structure of a Pol II–RNA inhibitor complex

We first mapped the minimal region of FC RNA required for Pol II interaction by partial hydrolysis and filter binding (Methods and **Fig. 1**). An RNA 33-mer corresponding to the mapped region (FC* RNA) bound Pol II with an affinity comparable to full-length FC RNA (K_d is 33 nM and 20 nM, respectively, for FC* and FC). FC* RNA was cocrystallized with the complete 12-subunit Pol II, and the X-ray structure was determined at 3.8-Å resolution (Methods). The RNA model was confirmed by bromine labeling and fits well to the initial unbiased difference electron density map (**Fig. 2**). The structure shows that FC* RNA binds in the polymerase active center cleft above the bridge helix[7] (**Fig. 3**). The RNA contacts the clamp and fork domains on opposite sides of the cleft (**Fig. 3b**), consistent with cross-linking of FC* RNA to the two large Pol II subunits[6]. Upon RNA binding, the cleft widens slightly (up to 2 Å, not shown), and polymerase-fork loops[7] 1 and 2 move by up to 7 and 14 Å, respectively (**Fig. 3c**). The RNA forms two stem-loop structures (**Fig. 2a,b**) with the two double strands twisted against each other. The 5′ stem and the 3′ stem contain 4 and 6 base pairs, respectively, of nearly A-form duplex. One RNA strand extends over both stems with continuous base stacking.

Analysis of Pol II–RNA interaction

The backbones of both RNA stems and most of the exposed bases of the 5′ loop contact Pol II extensively, whereas the 3′ loop is not bound and is mobile (**Fig. 2a,b**). About half the Pol II residues that contact RNA are not conserved in Pol I and Pol III of *S. cerevisiae* (**Fig. 2b**), explaining the specificity of FC RNA for inhibition of Pol II[6]. The relevance of the observed contacts for polymerase-RNA affinity was investigated by binding studies with mutant FC* RNAs (**Fig. 2c,d**). We observed that mutations of the contacted bases in the 5′ stem (mutants 1 and 5) and in the 5′ loop (mutants 2 and 3) decrease Pol II affinity,

[1]Gene Center, University of Munich, Department of Chemistry and Biochemistry, Feodor-Lynen-Str. 25, 81377 Munich, Germany. [2]Kekulé-Institut für Organische Chemie und Biochemie, Rheinische Friedrich-Wilhelms-Universität Bonn, Gerhard-Domagk-Straße 1, 53121 Bonn, Germany. [3]Current address: Max-Planck-Institute of Biochemistry, Department of Molecular Structural Biology, Am Klopferspitz 18, 82152 Martinsried, Germany. Correspondence should be addressed to M.F. (m.famulok@uni-bonn.de) or P.C. (cramer@LMB.uni-muenchen.de).

Received 27 September; accepted 3 November; published online 11 December 2005; doi:10.1038/nsmb1032

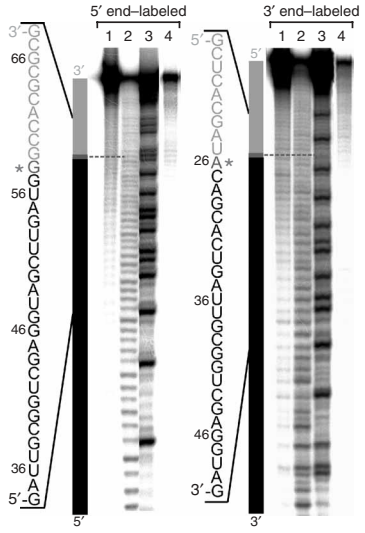

Figure 1 Mapping of the minimal Pol II-binding motif in FC RNA. Partially hydrolyzed variants of FC RNA were reselected for binding to yeast Pol II. Shown on the left is damage selection with the 5′ end–labeled full-length 80-mer FC RNA that was used to determine the 3′ border of the minimal motif. Lanes 1–4 show untreated full-length FC RNA, randomly digested RNA, an RNase T1 digest and a fraction of 5′-labeled fragments retained with yeast Pol II on nitrocellulose filters, respectively. Black, sequence required for binding; gray, sequence not required for binding. The bar shows the sequence in the linear scale of the gel with the same shading. G58 marks the 3′-terminal base. Shown on the right is damage selection with the 3′-labeled FC RNA that was used to determine the 5′ border of the minimal motif. Lanes are as in the left panel. A26 marks the 5′-terminal base according to the minimal length of retained fragments shown in lane 4.

as does extension of the 5′ stem (mutants 6 and 7) (**Fig. 2c,d**). These data are consistent with the contacts observed in the complex structure. None of the RNA mutations, however, is sufficient to abolish or even severely reduce the RNA-binding affinity. In contrast, a circular permutated RNA (**Fig. 2c,d**, mutant 9) does not bind Pol II, providing a negative control and indicating that the sharp twist between the two stems is crucial for the FC* RNA–polymerase interaction. Together, these results suggest that the global RNA structure is important for Pol II affinity and that a large number of Pol II-RNA contacts contribute to the overall affinity.

Structural comparison suggests the inhibitory mechanism

Comparison of our structure with structures of Pol II elongation complexes[8,9] reveals substantial overlap of the RNA inhibitor with nucleic acids in an elongation complex, and this explains why FC RNA inhibits initiation, but not elongation[6]. Binding of FC RNA to free Pol II blocks DNA entry into the polymerase cleft during initiation, hence the template cannot reach the active center and transcription cannot start (**Fig. 3a,b**). In a preformed elongation complex, however, nucleic acids tightly bound to an overlapping site exclude FC* RNA from the cleft (**Fig. 4a**). FC* RNA does not mimic nucleic acids in the elongation complex, although five backbone phosphate groups occupy equivalent positions, three at the upstream end of the DNA-RNA

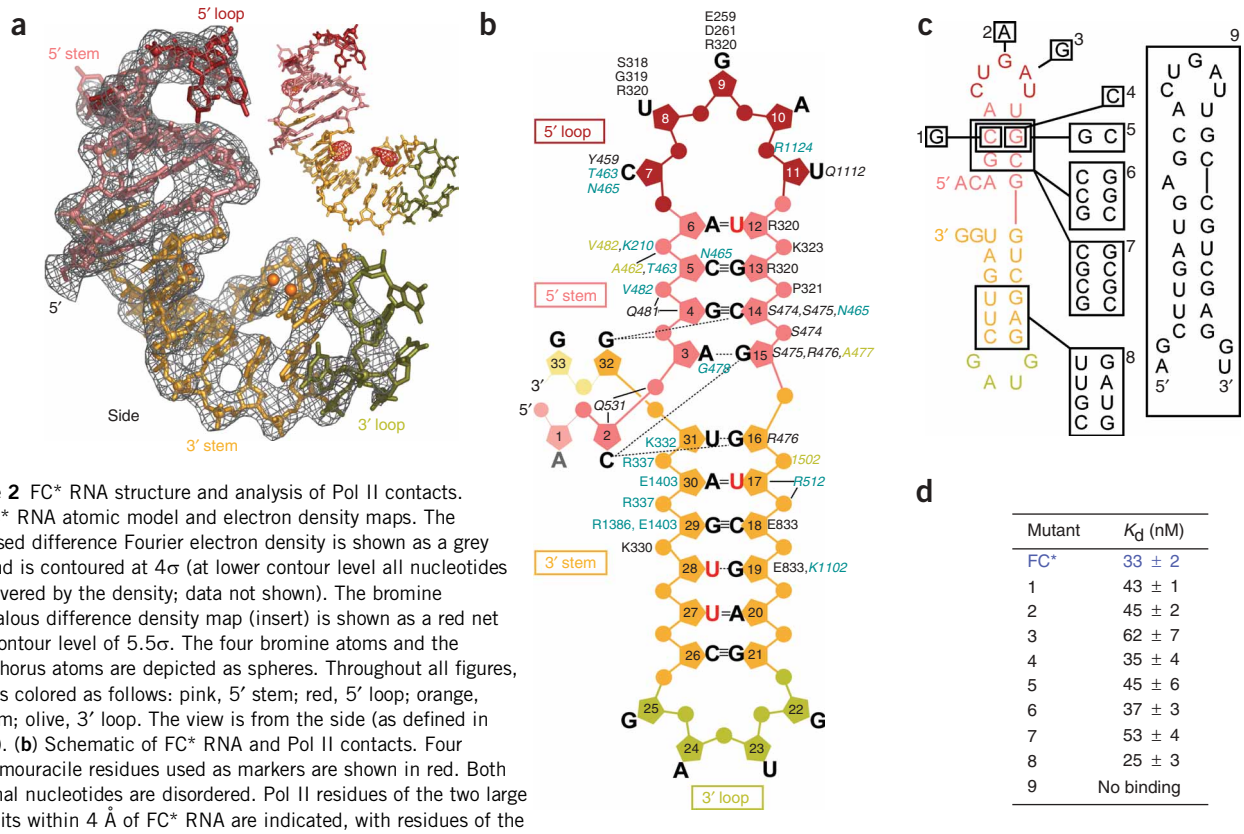

Mutant	K_d (nM)
FC*	33 ± 2
1	43 ± 1
2	45 ± 2
3	62 ± 7
4	35 ± 4
5	45 ± 6
6	37 ± 3
7	53 ± 4
8	25 ± 3
9	No binding

Figure 2 FC* RNA structure and analysis of Pol II contacts. (**a**) FC* RNA atomic model and electron density maps. The unbiased difference Fourier electron density is shown as a grey net and is contoured at 4σ (at lower contour level all nucleotides are covered by the density; data not shown). The bromine anomalous difference density map (insert) is shown as a red net at a contour level of 5.5σ. The four bromine atoms and the phosphorus atoms are depicted as spheres. Throughout all figures, RNA is colored as follows: pink, 5′ stem; red, 5′ loop; orange, 3′ stem; olive, 3′ loop. The view is from the side (as defined in ref. 7). (**b**) Schematic of FC* RNA and Pol II contacts. Four 5′-bromouracile residues used as markers are shown in red. Both terminal nucleotides are disordered. Pol II residues of the two large subunits within 4 Å of FC* RNA are indicated, with residues of the Rpb2 subunit in italics, and interactions with bases, phosphate groups or sugar moieties are distinguished. Cyan, residues invariant between *S. cerevisiae* Pol I, II and III; green, conserved residues; continuous and dashed lines, potential base-pair interactions. (**c**) Mutants of FC* RNA used for analysis of Pol II contacts. (**d**) Dissociation constants for the interaction of Pol II with the FC* RNA mutants in **c**, as determined by *in vitro* binding assays.

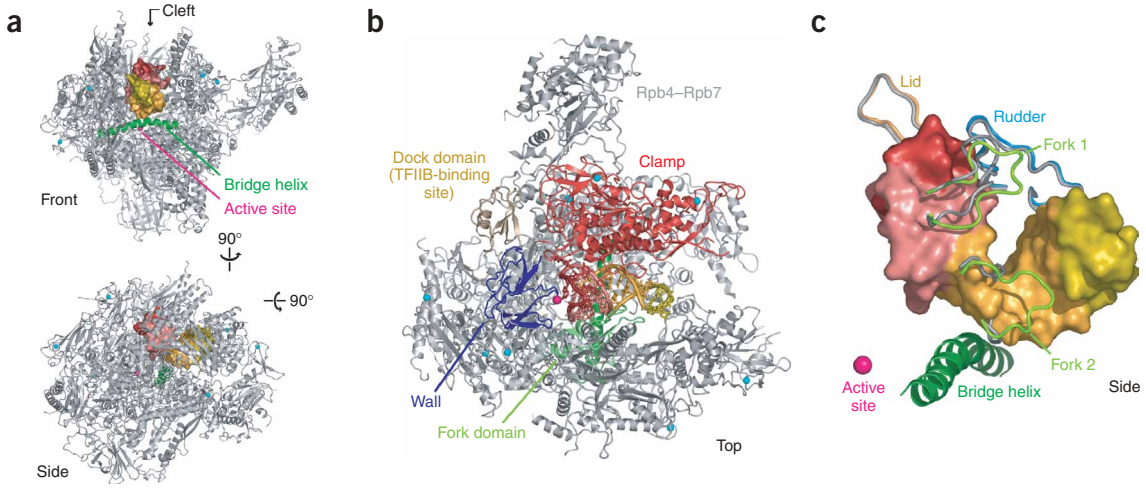

Figure 3 Structure of the Pol II–FC* RNA complex. The complete 12-subunit Pol II is shown as a ribbon model in silver and FC* RNA as a molecular surface colored as in **Figure 2**. (**a**) Two views[7] of the complex related by a 90° rotation around a vertical axis. Green, the bridge helix; pink sphere, the active site magnesium ion. (**b**) View of the structure from the top (as defined in ref. 7), with the clamp, fork, dock and wall domains highlighted. FC* RNA is shown as a stick model. (**c**) Structural response of Pol II to RNA binding. The view is from the side[7]. The Pol II structure has been removed for clarity, except for the rudder, lid and fork loops, which are shown in two conformations: as observed in a Pol II elongation complex structure[9] (grey) and as seen here in the Pol II–FC* RNA complex structure (colored). RNA binding induces large conformational changes in fork loops 1 and 2 (Rpb2 residues 467–477 and 502–509, respectively), by up to 7 and 14 Å, respectively.

hybrid and two in the template strand just before the active site (**Fig. 4a**). Despite the overlap, the RNA-binding site is distinct from the binding site for the DNA-RNA hybrid in an elongation complex. Only a subset of Pol II residues is involved in both interactions with the RNA inhibitor and with the DNA-RNA hybrid.

FC* RNA and B2 RNA compete for Pol II binding

Like FC RNA, B2 RNA inhibits initiation but not elongation[2], although these two RNAs do not share apparent sequence homology. This prompted us to ask whether FC RNA and B2 RNA bind and inhibit Pol II in a similar manner. We found that mouse B2 RNA prepared by *in vitro* transcription binds yeast Pol II as tightly as FC* RNA (K_d of 34 ± 2 nM and 33 ± 2 nM for B2 and FC* RNA, respectively), indicating that the B2 RNA-binding site on Pol II is conserved among eukaryotes. Competition experiments revealed that FC* RNA efficiently displaces B2 RNA from Pol II (**Fig. 4b**). Likewise, B2 RNA displaces FC* RNA prebound to Pol II (**Fig. 4b**). In contrast, a circular permutated FC* RNA mutant (**Fig. 2c,d**, mutant 9) did not compete efficiently with B2 or FC* RNA for Pol II binding, providing a negative control (**Fig. 4b**). Taken together, these data suggest that FC RNA and B2 RNA bind overlapping sites in the Pol II cleft. However, an alternative allosteric model for mutually competitive binding of the two RNAs to Pol II cannot be excluded.

DISCUSSION

Here we present the first structure of a multisubunit (cellular) RNA polymerase complexed with RNA alone, that of yeast Pol II bound to FC* RNA, the central part of an RNA aptamer that inhibits transcription initiation but not elongation. The structure shows the RNA bound to the Pol II cleft at a site that overlaps, but is not identical, with the binding site for nucleic acids in an elongation complex. This suggests that the RNA inhibitor prevents entry of promoter DNA

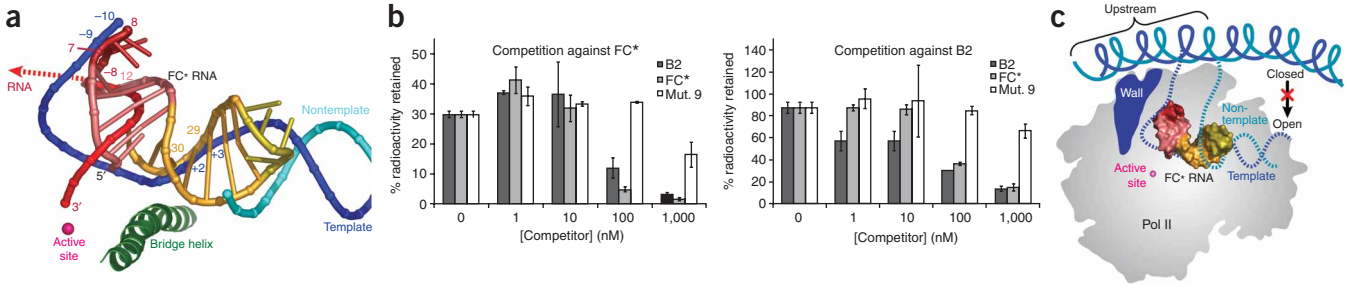

Figure 4 Model of RNA inhibition. (**a**) FC* RNA and nucleic acids in the Pol II elongation complex bind overlapping sites. The Pol II–FC* RNA complex structure was superimposed on the structure of the complete Pol II elongation complex[9]. Phosphate groups that occupy similar locations are labeled. The view is from the side (as defined in ref. 7). (**b**) Competition binding analysis suggests that FC* RNA and B2 RNA bind overlapping sites. Pol II complexes with radioactively labeled FC* RNA (top) or B2 RNA (bottom) were challenged with increasing concentrations of unlabeled competitor RNA as indicated. Mutant 9 was used as a negative control (**Fig. 1c**). See Methods for details. (**c**) Model for inhibition of open-complex formation by FC* RNA. The view is from the side[7]. The upstream region of the DNA promoter was placed on Pol II on the basis of its location in the bacterial RNA polymerase–promoter complex[13] and was extrapolated in the downstream direction. The downstream region of promoter DNA and the template strand in the bubble region of the open complex were modeled according to the complete Pol II elongation complex[9]. FC* RNA is shown as a molecular surface.

during initiation and that preformed elongation complexes are not inhibited because prebound nucleic acids in the cleft exclude the RNA inhibitor and cannot be displaced by it.

We further show that the natural RNA inhibitor B2 from mouse binds yeast Pol II and that B2 RNA and FC* RNA compete for Pol II binding. Thus, these RNAs may bind overlapping sites in the cleft and may use the same or a similar mechanism of inhibition. On the basis of this assumption, we predict a way in which promoter specificity of B2 RNA could arise. Studies in *Drosophila melanogaster* have shown that heat-shock genes contain preassembled elongation complexes stalled near the promoter[10], which are released upon heat activation[11]. According to our model, the stalled elongation complexes would be inert toward inhibition by B2 RNA because the RNA inhibitor would be excluded from the cleft by prebound nucleic acids. However, it is unclear how additional polymerases can initiate transcription of heat-shock genes in the presence of B2 RNA.

At which stage of the initiation pathway do RNA inhibitors act? Initiation starts with formation of a closed complex, in which the general transcription factor TFIIB forms a bridge between Pol II and promoter DNA above the cleft[12–16]. Upon DNA melting, the template single strand and the downstream DNA duplex enter the cleft, resulting in the open complex, and RNA synthesis commences. Superposition of our structure with the Pol II–TFIIB complex[17] shows that clashes are limited to the 'B-finger' of TFIIB and that FC* RNA would not interfere with binding of the TFIIB zinc-ribbon domain to the Pol II dock domain[7] (**Fig. 3b**). As the TFIIB zinc ribbon is essential for formation of the closed complex[18,19], we predict that FC* RNA does not prevent closed-complex formation. Instead, topological considerations suggest that FC* RNA prevents DNA entry into the cleft during open-complex formation (**Fig. 4c**). Consistent with this, FC RNA prevents Pol II binding to a 'tailed' DNA template[6], which mimics the template strand and the downstream DNA in an open complex.

As predicted for FC* RNA, B2 RNA can be incorporated into TFIIB-containing complexes[2] and therefore does not prevent closed-complex formation. As these B2 RNA–containing closed complexes are nonproductive[2], B2 RNA could prevent either open-complex formation or the transition from an open to an elongation complex. Thus, all current evidence is consistent with the model where both RNAs do not inhibit closed-complex formation, but prevent formation of the open complex.

Finally, the bacterial transcription inhibitor 6S RNA has been suggested to mimic melted promoter DNA in an open complex, as it forms a duplex with a bubble that is required for polymerase binding[3–5]. For open-complex mimicry, A-form regions in 6S RNA must replace B-form DNA flanking the bubble. Our structure shows that an A-form RNA duplex, the 3′ stem of FC*, can bind the cleft with the same polarity as downstream DNA. This site could accommodate a longer RNA duplex, as in 6S RNA, as extension of the 3′ stem is sterically possible (**Fig. 3b**) and does not decrease the affinity of FC* for Pol II (**Fig. 2c,d**, mutant 8). Two of the phosphate groups in the 3′ stem superimpose with the DNA-template phosphates at positions +3 and +2 (**Fig. 4a**), so it is topologically feasible that one RNA strand continues into the active center, mimicking the template strand in an open complex, as suggested for 6S RNA[3–5]. This model awaits confirmation by the structure of a bacterial RNA polymerase bound to 6S RNA.

METHODS

RNA-protein interactions. Endogenous core Pol II from *S. cerevisiae* and recombinant Rpb4–Rpb7 subcomplex were purified as described in ref. 14. DNA corresponding to FC* RNA constructs was obtained using standard PCR and primers with the desired modifications. RNAs were obtained by *in vitro* transcription with T7 RNA polymerase (Fermentas). 5′ ^{32}P-labeled RNA (0.5 nM) was incubated with increasing concentrations (1–1,000 nM) of Pol II in buffer A (50 mM Tris-HCl (pH 7.4), 60 mM ammonium sulfate, 10 μM $ZnCl_2$, 5 mM Tris-(2-carboxyethyl)phosphine) in the presence of tRNA (2.5 μg ml^{-1}) for 30 min at 30 °C. RNA–protein complexes were retained on 0.45-μm nitrocellulose filters and washed with 300 μl of buffer A. The amounts of bound RNA were determined by phosphorimager quantification. For filter-binding competition assays, 5′ ^{32}P-labeled RNA was incubated with 100 nM protein under the same conditions, adding increasing amounts (1–1,000 nM) of unlabeled RNA competitor and then incubating at 30 °C for 30 min.

Mapping of RNA minimal motif. 5′ or 3′ ^{32}P-labeled RNA (0.5 pmol) was subjected to partial alkaline hydrolysis in 50 mM $NaHCO_3$ (pH 9.2) and 1 mM EDTA at 95 °C for 10 min. RNA was precipitated, dissolved in 30 μl H_2O and used in filter-binding assays as above. RNA retained on the filter was eluted with 30 mM Tris-HCl (pH 7.5), 6 M guanidine hydrochloride and 5 mM EDTA, then precipitated, dissolved in loading buffer and run on a denaturing 12% PAGE gel.

Crystal structure determination. The Pol II–RNA complex was reconstituted by incubating yeast core Pol II with a 5-fold molar excess of recombinant Rpb4–Rbp7 (ref. 14) and a 1.5-fold molar excess of synthetic FC* RNA containing 5-bromouracil at positions 12, 17, 27 and 28 (biomers.net) in 50 mM HEPES (pH 7.5), 40 mM ammonium sulfate, 5 μM $ZnCl_2$, 5% (v/v) glycerol and 10 mM DTT for 15 min at 20 °C. The complex was purified by gel filtration (Superose 6 HR, Amersham) in 5 mM HEPES (pH 7.25), 40 mM ammonium sulfate, 10 μM $ZnCl_2$ and 10 mM DTT, and was concentrated to 4 mg ml^{-1} before FC* RNA was added to a final concentration of 2 μM. Crystals were grown, harvested, cryo-protected and flash-frozen as described in ref. 9. The presence of RNA in the crystals was detected with a newly designed fluorescence-based assay[20]. Diffraction data (**Table 1**) were collected in 0.25° increments at beamline X06SA of the Swiss Light Source at a wavelength of 0.919 Å and were processed with HKL2000 (ref. 21). The crystal showed a mosaicity of 0.3–0.6° which was refined in segments of five frames. The structure was solved by molecular replacement with the structure of the complete 12-subunit Pol II[22] using PHASER[23]. After rigid-body refinement with CNS[24], an $F_o - F_c$ difference Fourier map showed continuous electron density for the RNA, and bromine positions were revealed in an anomalous

Table 1 Data collection and refinement statistics

Data collection	
Space group	$C222_1$
Cell dimensions	
a, *b*, *c* (Å)	224.6, 399.8, 286.7
Resolution (Å)	50–3.8 (3.9–3.8)
R_{sym}	13.9 (36.7)
$I/\sigma I$	12.2 (3.2)
Completeness (%)	99.9 (99.7)
Redundancy	6.1 (5.2)
Refinement	
Resolution (Å)	3.8
No. reflections	129,311
R_{work} / R_{free}	25.3/27.6
No. atoms	
Protein	31,081
Ligand/ion	8 (Zn^{++}), 666 (RNA)
B-factors	
Protein	99.0
Ligand/ion	84.8 (Zn^{++}), 113.0 (RNA)
R.m.s. deviations	
Bond lengths (Å)	0.001
Bond angles (°)	1.6

Highest resolution shell is shown in parentheses.

difference Fourier map (**Fig. 2a**). Positional and *B*-factor refinement of the complex (using CNS), excluding FC* residues 22–25, was monitored by a free *R*-factor calculated from a set of reflections excluded in the refinement of the free Pol II structure[22]. A difference electron density map, phased with the free Pol II structure, allowed building of an atomic model for the 33-mer FC* RNA, except the two terminal residues, which are disordered.

Preparation of B2 RNA. A DNA fragment was assembled from overlapping oligonucleotides containing nucleotides 1–149 of the mouse B2 RNA gene (178 bp, region 121488–121665 of *Mus musculus* chromosome 18, clone RP23-6p18, GenBank accession number AC020972). The sequences of the oligonucleotides were as follows: 5′-ATTCTAATACGACTCACTATAGGGCTGGTGAGATGGCTCAGTGGG-3′, 5′-TAAGAGCACCCGACTGCTCTTCCGAAGGTCAGGAGTTCAAATCCCAGC-3′, 5′-AACCACATGGTGGCTCACAACCATCCGTAACGAGATCTGATTCCCTC-3′ and 5′-TTCTGGAGTGTCTGAAGACAGCTACAGTGT-3′ (coding strand); 5′-TCTCACCAGCCCTATAGTGAGTCGTATTAG-3′, 5′-ACTCCTGACCTTCGGAAGAGCAGTCGGGTGCTCTTACCCACTGAGCCA-3′, 5′-TCTCGTTACGGATGGTTGTGAGCCACCATGTGGTTGCTGGGATTTGG-3′ and 5′-CTAGACACTGTAGCTGTCTTCAGACACTCCAGAAGAGGGAATCAGA-3′ (noncoding strand). The fragment contained a T7 promoter upstream of the B2 sequence and EcoRI and XbaI overhangs at the upstream and downstream ends, respectively. This construct was introduced into a pEBFP vector to yield plasmid pUC19-B2-1-149. For runoff transcription, DNA templates were obtained by digesting pUC19-B2-1-149 with XbaI and purifying the DNA by phenol-chloroform extraction. The transcription reaction contained 40 mM Tris-HCl (pH 8.0), 5 mM DTT, 1 mM spermidine, 0.01% (v/v) Triton X100, 4 mM each of ATP, GTP, UTP and CTP, 30 mM $MgCl_2$, 0.1 mg ml^{-1} linear DNA and 10 μg ml^{-1} T7 RNA polymerase. Reactions were incubated for 4 h at 37 °C. B2 RNA was purified by 8% (w/v) denaturing PAGE.

Accession codes. Protein Data Bank: Coordinates have been deposited with accession code 2B63.

ACKNOWLEDGMENTS

We thank C. Schulze-Briese and the staff of beamline X06SA at the Swiss Light Source for help. We thank O. Weichenrieder for advice on cloning and *in vitro* transcription of B2 RNA. M.F. and P.C. are supported by the Deutsche Forschungsgemeinschaft, the European Union and the Fonds der Chemischen Industrie.

COMPETING INTERESTS STATEMENT

The authors declare that they have no competing financial interests.

Published online at http://www.nature.com/nsmb/
Reprints and permissions information is available online at http://npg.nature.com/reprintsandpermissions/

1. Allen, T.A., Von Kaenel, S., Goodrich, J.A. & Kugel, J.F. The SINE-encoded mouse B2 RNA represses mRNA transcription in response to heat shock. *Nat. Struct. Mol. Biol.* **11**, 816–821 (2004).
2. Espinoza, C.A., Allen, T.A., Hieb, A.R., Kugel, J.F. & Goodrich, J.A. B2 RNA binds directly to RNA polymerase II to repress transcript synthesis. *Nat. Struct. Mol. Biol.* **11**, 822–829 (2004).
3. Trotochaud, A.E. & Wassarman, K.M. A highly conserved 6S RNA structure is required for regulation of transcription. *Nat. Struct. Mol. Biol.* **12**, 313–319 (2005).
4. Wassarman, K.M. & Storz, G. 6S RNA regulates *E. coli* RNA polymerase activity. *Cell* **101**, 613–623 (2000).
5. Barrick, J.E., Sudarsan, N., Weinberg, Z., Ruzzo, W.L. & Breaker, R.R. 6S RNA is a widespread regulator of eubacterial RNA polymerase that resembles an open promoter. *RNA* **11**, 774–784 (2005).
6. Thomas, M. *et al.* Selective targeting and inhibition of yeast RNA polymerase II by RNA aptamers. *J. Biol. Chem.* **272**, 27980–27986 (1997).
7. Cramer, P., Bushnell, D.A. & Kornberg, R.D. Structural basis of transcription: RNA polymerase II at 2.8 angstrom resolution. *Science* **292**, 1863–1876 (2001).
8. Westover, K.D., Bushnell, D.A. & Kornberg, R.D. Structural basis of transcription: nucleotide selection by rotation in the RNA polymerase II active center. *Cell* **119**, 481–489 (2004).
9. Kettenberger, H., Armache, K.-J. & Cramer, P. Complete RNA polymerase II elongation complex structure and its interactions with NTP and TFIIS. *Mol. Cell* **16**, 955–965 (2004).
10. Rasmussen, E.B. & Lis, J.T. *In vitro* transcriptional pausing and cap formation on three *Drosophila* heat shock genes. *Proc. Natl. Acad. Sci. USA* **90**, 7923–7927 (1993).
11. Lis, J. Promoter-associated pausing in promoter architecture and postinitiation transcriptional regulation. *Cold Spring Harb. Symp. Quant. Biol.* **63**, 347–356 (1998).
12. Chung, W.H. *et al.* RNA polymerase II/TFIIF structure and conserved organization of the initiation complex. *Mol. Cell* **12**, 1003–1013 (2003).
13. Murakami, K.S., Masuda, S., Campbell, E.A., Muzzin, O. & Darst, S.A. Structural basis of transcription initiation: an RNA polymerase holoenzyme-DNA complex. *Science* **296**, 1285–1290 (2002).
14. Armache, K.-J., Kettenberger, H. & Cramer, P. Architecture of the initiation-competent 12-subunit RNA polymerase II. *Proc. Natl. Acad. Sci. USA* **100**, 6964–6968 (2003).
15. Chen, H.T. & Hahn, S. Mapping the location of TFIIB within the RNA polymerase II transcription preinitiation complex: a model for the structure of the PIC. *Cell* **119**, 169–180 (2004).
16. Bushnell, D.A. & Kornberg, R.D. Complete RNA polymerase II at 4.1 Å resolution: implications for the initiation of transcription. *Proc. Natl. Acad. Sci. USA* **100**, 6969–6972 (2003).
17. Bushnell, D.A., Westover, K.D., Davis, R.E. & Kornberg, R.D. Structural basis of transcription: an RNA polymerase II-TFIIB cocrystal at 4.5 Angstroms. *Science* **303**, 983–988 (2004).
18. Buratowski, S. & Zhou, H. Functional domains of transcription factor TFIIB. *Proc. Natl. Acad. Sci. USA* **90**, 5633–5637 (1993).
19. Pardee, T.S., Bangur, C.S. & Ponticelli, A.S. The N-terminal region of yeast TFIIB contains two adjacent functional domains involved in stable RNA polymerase II binding and transcription start site selection. *J. Biol. Chem.* **273**, 17859–17864 (1998).
20. Kettenberger, H. & Cramer, P. Fluorescence detection of nucleic acids and proteins in multicomponent crystals. *Acta Crystallogr. D Biol. Crystallogr* (in the press).
21. Otwinowski, Z. & Minor, W. Processing of X-ray diffraction data collected in oscillation mode. *Methods Enzymol.* **276**, 307–326 (1996).
22. Armache, K.-J., Mitterweger, S., Meinhart, A. & Cramer, P. Structures of complete RNA polymerase II and its subcomplex Rpb4/7. *J. Biol. Chem.* **280**, 7131–7134 (2005).
23. McCoy, A.J., Grosse-Kunstleve, R.W., Storoni, L.C. & Read, R.J. Likelihood-enhanced fast translation functions. *Acta Crystallogr. D Biol. Crystallogr.* **61**, 458–464 (2005).
24. Brunger, A.T. *et al.* Crystallography & NMR system: A new software suite for macromolecular structure determination. *Acta Crystallogr. D Biol. Crystallogr.* **54**, 905–921 (1998).